Kinetics and Thermodynamics of the Interchange of the Morpheein Forms of Human Porphobilinogen Synthase[†]

Trevor Selwood, Lei Tang, Sarah H. Lawrence, Yana Anokhina, and Eileen K. Jaffe*

Fox Chase Cancer Center, 333 Cottman Avenue, Philadelphia, Pennsylvania 19111

Received October 19, 2007; Revised Manuscript Received December 7, 2007

ABSTRACT: A morpheein is a homo-oligomeric protein that can adopt different nonadditive quaternary assemblies (morpheein forms) with different functionalities. The human porphobilinogen synthase (PBGS) morpheein forms are a high activity octamer, a low activity hexamer, and two structurally distinct dimer conformations. Conversion between hexamer and octamer involves dissociation to dimers, conformational change at the dimer level, followed by association to the alternate assembly. The current work promotes an alternative and novel view of the physiologically relevant dimeric structures, which are derived from the crystal structures, but are distinct from the asymmetric units of their crystal forms. Using a well characterized heteromeric system (WT+F12L; Tang, L. et al. (2005) *J. Biol. Chem. 280*, 15786–15793), extensive study of the human PBGS morpheein reequilibration process now reveals that the intervening dimers do not dissociate to monomers. The morpheein equilibria of wild type (WT) human PBGS are found to respond to changes in pH, PBGS concentration, and substrate turnover. Notably, the WT enzyme is predominantly an octamer at neutral pH, but increasing pH results in substantial conversion to lower order oligomers. Most significantly, the free energy of activation for the conversion of WT+F12L human PBGS heterohexamers to hetero-octamers is determined to be the same as that for the catalytic conversion of substrate to product by the octamer, remarkably suggesting a common rate-limiting step for both processes, which is postulated to be the opening/closing of the active site lid.

Studies on porphobilinogen synthase (PBGS[1], EC 4.2.1.24) have resulted in the introduction of the term morpheein to describe a homo-oligomeric protein that exists as an equilibrium of functionally distinct, nonadditive quaternary structural isoforms (morpheein forms) (*1*). The morpheein forms of human PBGS are an octamer, a hexamer, and two different dimer conformations (Figure 1a) wherein the interconversion of hexamer and octamer must involve dissociation to dimers. The dimer adopts conformations (Figure 1b) that dictate whether assembly will be to the octamer or the hexamer. The response of these equilibria to the protein's environment or allosteric regulator molecules can serve a regulatory function (*1*). Notably, naturally occurring mutations that affect the hexamer−octamer equilibria have been linked to the human disease porphyria (*2*). The reader may note that the pro-octamer and pro-hexamer dimers depicted in Figure 1 supersede the previously described hugging and detached dimers, which are the asymmetric units of the crystal structures of the human WT octamer and F12L hexamer, respectively (*1, 3–5*). The new dimer structures are derived from the same crystal structures, but pair monomers from adjacent dimeric asymmetric units. Consideration of these alternate dimers is consistent with rising evidence that the asymmetric unit of a crystal structure need not reflect the physiologically relevant fundamental structural unit (*6, 7*). Notable is the unexpected structure of the physiologically relevant dimer of sulfotransferase (*6*).

Prior characterizations of wild type (WT) human PBGS at neutral pH demonstrated it to be predominantly octameric with high activity and a K_m in the range of the physiologic concentration of substrate (*3*). However, kinetic characterization of WT human PBGS in the alkaline pH range indicated the appearance of an additional higher K_m form (*3, 5*). Conversely, the naturally occurring F12L variant behaves as a stable hexamer with low activity at neutral pH and high K_m values at all pH values (Figure 1c) (*3*). The most obvious difference between the subunits that comprise the octamer versus the hexamer is the orientation of the N-terminal arm relative to the $\alpha\beta$-barrel (Figure 1d); differences also exist in order/disorder in the region surrounding the active site (Figure 1e). Notably, both crystal structures of the human PBGS oligomers reveal the occupancy of half of the sites for the substrate-derived active site ligands; in both the WT octamer and the F12L hexamer, the unoccupied active sites contain a disordered active site lid.

The PBGS-catalyzed reaction is an asymmetric condensation of two molecules of 5-aminolevulinic acid (ALA; 5-amino-4-oxo-hepatanoic acid). The WT human PBGS octamer reaction mechanism is briefly described as follows (*8*). The first ALA binds deep in the active site and forms a

[†] This work was supported by NIH Grants ES03654 (to E.K.J.), CA006927 (Institute for Cancer Research), and CA009835 (Fox Chase Cancer Center), and by an appropriation from the Commonwealth of Pennsylvania.

* Corresponding author. Eileen K. Jaffe, Fox Chase Cancer Center, 333 Cottman Avenue, Philadelphia, PA 19111. Tel: 215-728-3695. Fax: 215-728-2412. E-mail: Eileen.Jaffe@fccc.edu.

[1] Abbreviations: ALA, 5-aminolevulinic acid; BME, 2-mercaptoethanol; BTP-HCl, 1,3-bis[tris(hydroxymethyl)methylamino]propane hydrochloride; PBGS, porphobilinogen synthase; PAGE, polyacrylamide gel electrophoresis; SEC, size exclusion chromatography; TCEP, tris(2-carboxyethyl)phosphine; WT, wild type.

10.1021/bi702113z CCC: $40.75
Published on Web 02/14/2008

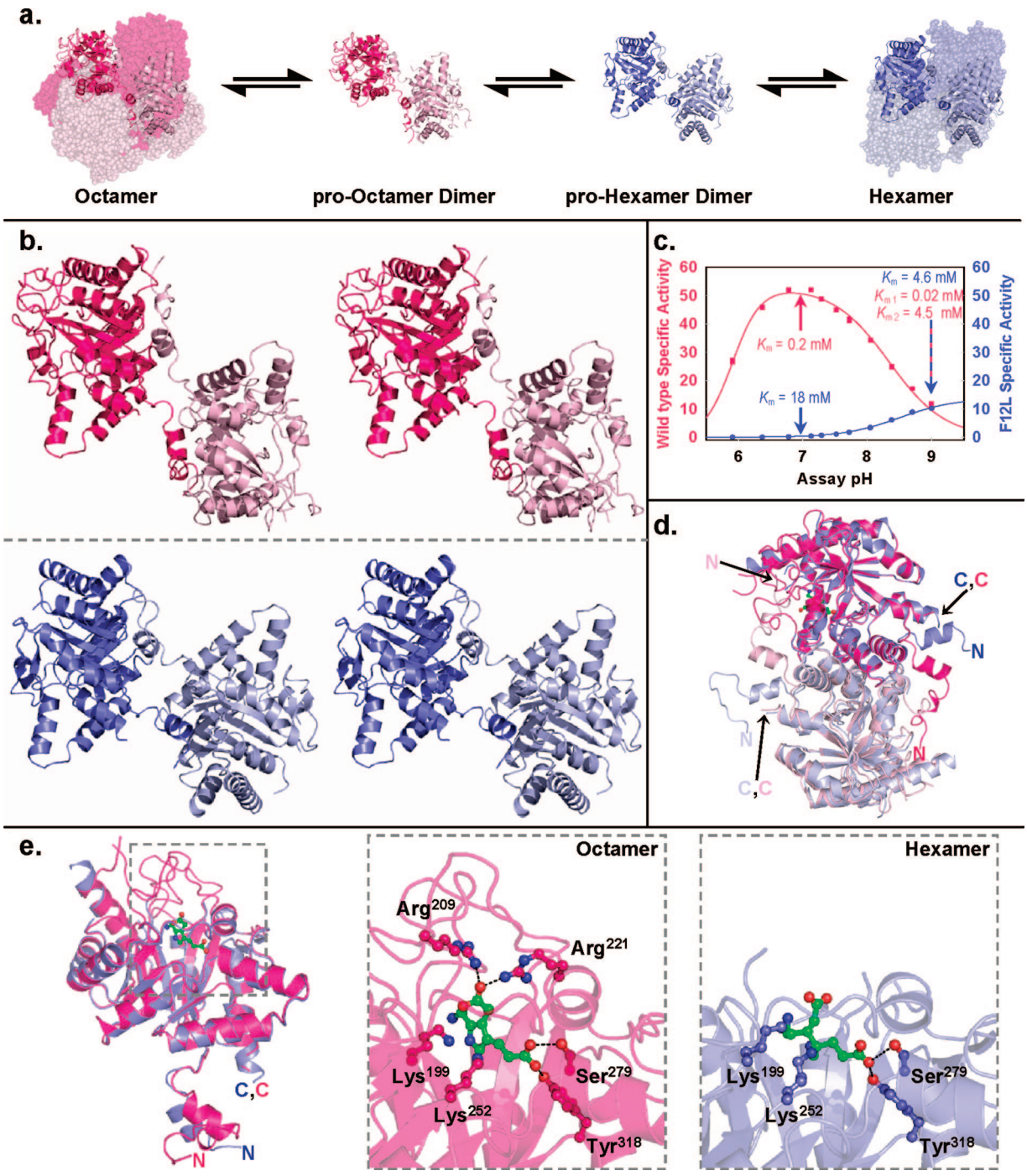

FIGURE 1: Structural and kinetic characteristics of the morpheein forms of human PBGS. (a) The inherent asymmetry of human PBGS homo-oligomers is illustrated throughout by light chains and dark chains. The human PBGS octamer (PDB code: 1E51) is assembled from four pro-octamer dimers. The pro-octamer dimers exist in equilibrium with the structurally distinct pro-hexamer dimers, three of which assemble to form the hexamer (PDB code: 1PV8 which is the F12L variant). The chains of the octamer and pro-octamer dimer are colored in shades of pink. The chains of the hexamer and pro-hexamer dimer are colored in shades of blue. The structures of the pro-octamer and pro-hexamer dimer derive from the crystals structures 1E51 and 1PV8, respectively, but are not equivalent to the asymmetric units, each of which is an A/B (light/dark) dimer. The pro-octamer and pro-hexamer dimers comprise the A subunit of one asymmetric unit and the B subunit of the adjacent asymmetric unit. (b) Stereo view illustrating the conformational differences between the pro-octamer (top) and pro-hexamer (bottom) dimers. The A chains of the dimers (dark pink and dark blue) are oriented identically. (c) The pH activity profiles of WT (pink) and F12L (blue) human PBGS (37 °C, 10 mM ALA-HCl), annotated with the pH dependent K_m values for these two variants. (d) An overlay of the asymmetric units of the octamer (light and dark pink) and hexamer (light and dark blue) crystal structures. This orientation emphasizes the different conformations of the N-terminal arms with respect to the $\alpha\beta$-barrel domains and also shows that only one of the four subunits displayed contains an ordered active site lid (also see part e). (e) An overlay of the A chains of the octamer (pink) and hexamer (blue) crystal structures, each of which contains an active site ligand (only porphobilinogen is shown). The zoomed-in panels show details of the active sites in the octamer and the hexamer. Porphobilinogen, shown with the carbons colored green, was modeled to the electron density seen in the active site of the octamer structure (*22*) and is shown to interact with a closed conformation of the active site lid. The density in the hexamer active site was modeled to contain 3-(2-aminoethyl)-4(aminomethyl)heptanedioic acid (*3*), also shown with the carbons colored green, and the active site lid is disordered.

Schiff base to Lys252. The second ALA then binds, and its carboxyl group interacts with basic residues on the active site lid, helping to secure a closed lid conformation (Figure 1e). Significant chemistry occurs in the closed active site, including the formation of one or more additional Schiff base intermediates. The crystal structure of hexameric F12L PBGS shows that interaction with the second ALA is insufficient to secure the closed lid environment (Figure 1e), leaving an exposed active site that requires high solvent pH to facilitate the additional Schiff base formation (Figure 1c). The absence of the lid interactions with the K_m-determining second substrate results in a K_m value for the hexamer that is much higher than the K_m value for the octamer (Figure 1c). Of the four assemblies illustrated in Figure 1a, only the octamer has the specific arm-to-barrel interface that assists the second substrate in stabilizing the closed conformation of the active site lid (see Discussion). Consequently, the pro-octamer and pro-hexamer dimers are predicted to require high pH for activity and to exhibit high K_m values. These kinetic characteristics have already been observed for the dimeric human PBGS variant W19A, which does not form higher-order oligomers (*4*); however, the precise structures of the W19A dimers have not been determined.

Interconversion of the high activity octamer and the low activity hexamer via the dissociation, conformational change, association mechanism depicted in Figure 1a has been established using WT+F12L hetero-oligomers that were prepared by heterologous coexpression of WT and F12L PBGS in *Escherichia coli* (*3, 5*) which is also used herein. This coexpression produces a mixture of heterohexamers and hetero-octamers that can be separated by ion exchange chromatography. Both hetero-oligomers contain subunits with Phe12 and Leu12. The hetero-oligomers are metastable in that their interchange does not occur readily but can be facilitated by substrate turnover (*5*), which shifts the equilibria to favor the octamer. Reequilibration of heterohexamers and hetero-octamers during catalytic turnover is accompanied by a disproportionation of the subunits wherein the Phe12-containing subunits accumulate in the octamer, and the Leu12-containing subunits accumulate in the hexamer (*5*). The subunit disproportionation establishes that interconversion involves a dynamic disassembly and reassembly of the oligomeric forms. The current study uses this system to address the rate-limiting activation energy for heterohexamer to hetero-octamer conversion and to address whether the dimers dissociate to monomers during this process.

The prior observation of a high K_m form of WT human PBGS at alkaline pH suggests that its morpheein equilibria are also dynamic, akin to the now well characterized WT+F12L system (*1, 3, 5*). The current study addresses the WT human PBGS high K_m forms, which are found to be the result of a rapid response of the morpheein equilibria to pH, PBGS concentration, and substrate turnover. The energy barriers to the interconversion of human PBGS morpheein forms are found to be small but not equal to each other, and the rate-limiting process is a conformational change rather than an assembly or disassembly process. A comparative thermodynamic analysis of the WT+F12L hetero-oligomer interconversion relative to catalysis by homo-octameric, hetero-octameric, and homohexameric assemblies of human PBGS reveals the importance of conformational changes in PBGS catalysis.

EXPERIMENTAL PROCEDURES

Genes and Constructs. The plasmids for human PBGS N59/C162A (WT), the F12L variant, and the plasmid for coexpressed WT+F12L using two promoters were described elsewhere (*3, 4, 9*).

Protein Expression and Purification. Plasmids were transformed into *E. coli* BLR (DE3) cells for protein expression. The proteins were purified from the soluble fraction of the lysed cells using 20–45% ammonium sulfate fractionation, hydrophobic chromatography on phenyl-Sepharose, anion-exchange chromatography on Q-Sepharose, and size exclusion chromatography (SEC) on Sephacryl S-300 as described elsewhere (*3, 9*). Protein concentrations were determined by the Bradford assay (Pierce, Rockford, IL) using bovine serum albumin as the standard.

The WT+F12L hetero-oligomers were produced by heterologous expression in *E. coli* using a two promoter plasmid as we have done previously (*3, 5*). Heterohexamers and hetero-octamers were separated using anion exchange chromatography on a Q-Sepharose column. Fractions were pooled on the basis of their specific activities at pH 7.0 and pH 9.0 and native PAGE analyses. For each pool, the final purification step was SEC on Sephacryl S-300. Native PAGE showed that one pool contained almost exclusively heterohexamer (*5*). This sample was used as the starting point for all of the heterohexamer to hetero-octamer conversion experiments described herein.

PBGS Activity Determination. Enzyme activity was based on the measurement of porphobilinogen formed from ALA by PBGS, using specific activity units of μmol porphobilinogen h^{-1} mg^{-1}. Assay buffer was 0.1 M 1,3-bis[tris(hydroxymethyl)methylamino]propane hydrochloride (BTP-HCl) at desired pH values, 10 mM 2-mercaptoethanol (BME) or 1 mM Tris(2-carboxyethyl)phosphine hydrochloride (TCEP-HCl), and 10 μM $ZnCl_2$. The reported pH values, which are generally 0.2–0.3 pH units below the preincubation conditions, reflect the assay pH after the addition of 0.1 M ALA hydrochloride (ALA-HCl) to a final concentration of 10 mM and 1 mM TCEP-HCl (when used). At concentrations of ALA-HCl < 10 mM, the final pH was maintained by diluting stock ALA-HCl (normally at 0.1 M) into 0.1 M HCl. Assays were performed at 37 °C unless otherwise stated. The production of porphobilinogen was determined using two methods.

The first method, referred to as Ehrlich's assay, quantifies the complex formed between porphobilinogen and Ehrlich's reagent (2 g *p*-(dimethylamino)benzaldehyde, 80 mL glacial acetic acid, and 20 mL of 70% perchloric acid) (ε = 60,200 $M^{-1}cm^{-1}$ at 555 nm) (*10*). Typically, the assay volume was 1.0 mL, and, unless stated otherwise, the enzyme was preincubated in 0.9 mL assay buffer at 37 °C for 10 min before the addition of 0.1 mL ALA-HCl. For the Ehrlich's assay, the reducing agent was BME, and the reaction was stopped with 0.5 mL of 20% trichloroacetic acid and 0.1 M $HgCl_2$; this terminates the reaction and precipitates both protein and BME. Colorometric determination of porphobilinogen was as previously described (*5*).

The second method, referred to in the text as the 236 nm assay, monitored the production of porphobilinogen via its absorbance at 236 nm (ε = 5,500 $M^{-1}cm^{-1}$ (*11*)) using a Cary 50 Bio spectrophotometer (Varian Inc.) equipped with

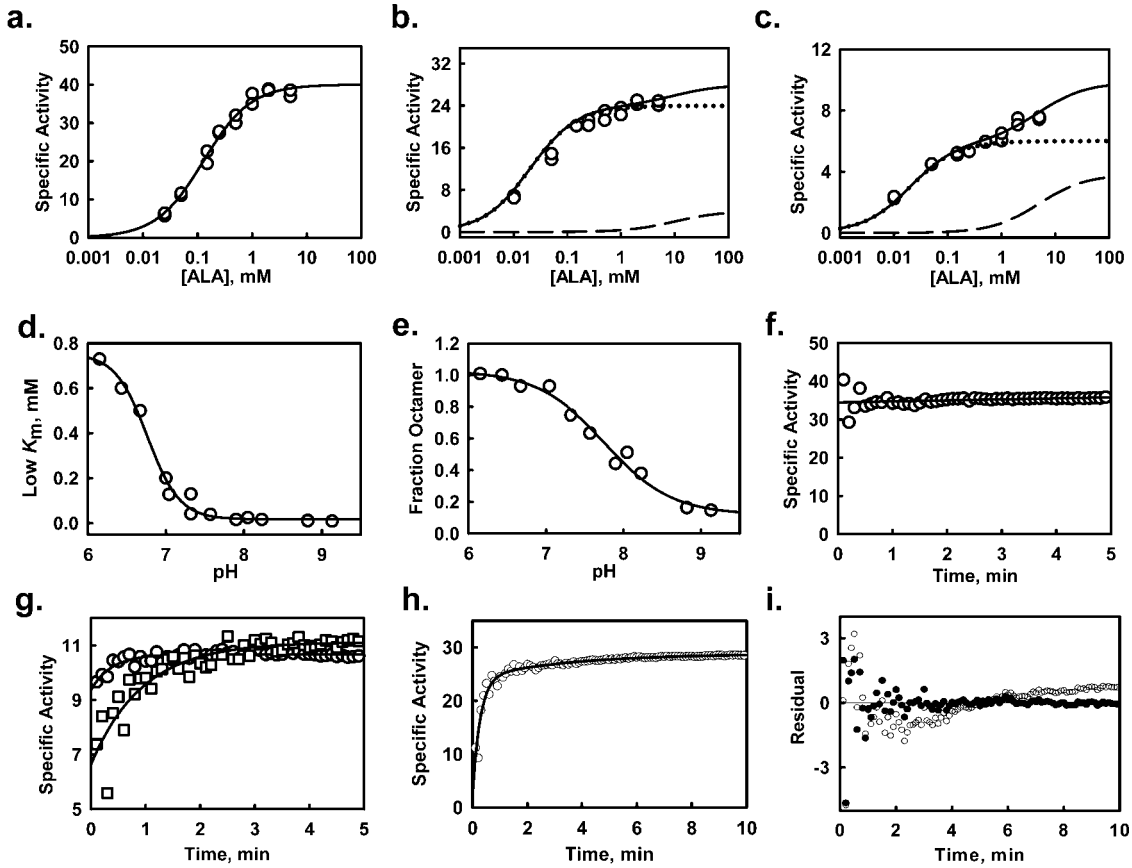

FIGURE 2: Kinetic analysis of WT human PBGS indicates the morpheein equilibrium. (a) A plot of specific activity vs substrate concentration obtained at pH 7.0 ([WT PBGS] = 5 μg/mL) using 1 mL, 5 min Ehrlich's assays. Reactions were initiated by the addition of enzyme (<50 μL). The solid line is a fit of the data to the standard hyperbolic Michaelis–Menten equation (eq 1). (b) A similar plot at pH 8.0 ([WT PBGS] = 10 μg/mL). (c) A similar plot at pH 8.8 ([WT PBGS] = 20 μg/mL).The solid lines in panels b and c were obtained by modeling the double hyperbolae using eqs 2 and 3 (see text). The dotted line shows the fitted contributions from the low K_m octamer, and the dashed line shows the fitted contribution from the high K_m species. (d) The fitted values for K_{m1} as a function of pH fit best to a two proton pK_a value of 6.8 (eq 7). (e) The fraction of octamer (V_{max1}/40) was estimated from the kinetic parameters, which were determined as per parts b and c, over the pH range from 6.2–9.5. The presented fit is to a single one proton pK_a value (eq 7). (f) The 236 nm assay of WT PBGS (10 μg/mL) at pH 6.9, where the reaction is initiated by addition of ALA-HCl to 1 mM. (g) The 236 nm assay of WT PBGS at pH 8.8. The concentrations of enzyme were 30 μg/mL (□) and 100 μg/mL (○). The solid lines are fits to the data obtained using eq 4. Apart from the pH and enzyme concentration the conditions used were the same as those used in part f. (h) Specific activity time courses upon transferring WT human PBGS from pH 9.0 to pH 7.0 (○) and fitted to a double exponential function (eq 5). (i) A plot of residuals for the single (○) vs double (●) exponential fit to the data presented in part h.

a thermostatted multicuvette holder connected to a circulating water bath. The temperature was monitored via a probe in a water filled cuvette adjacent to the reaction cuvette. TCEP-HCl (1 mM) was used instead of 10 mM BME as the reducing agent to minimize background absorbance. To account for any background absorbance and nonenzymatic condensation of substrate, control time courses without enzyme were subtracted from the reaction time courses. Specific activities reported in Figure 2f–h were calculated on the basis of the increase in absorbance between time 0 and the indicated time.

Analytical Size Exclusion Chromatography. The oligomeric forms of WT PBGS were analyzed by SEC on a Superdex 200 (GE Healthcare) using 0.1 M BTP-HCl at pH 8.8, 0.1 M KCl, 10 mM HCl, 1 mM TCEP-HCl and 10 μM $ZnCl_2$, at 1 mL/min, and at room temperature. The protein (1 mg/mL, same buffer, 100 μL) was loaded in a 100 μL injection loop following a 10 min. incubation at 37 °C. Protein elution was monitored at 280 nm using a GE Healthcare UPC-900 detector. The chromatograph was deconvoluted using the residuals mode in the program PeakFit (Jandel Scientific). High protein concentration, ~1 mg/mL, was required for meaningful quantitation of the minor components (hexamer and dimer).

Anion Exchange Chromatography Analyses of WT Human PBGS. Anion exchange chromatography was performed using a Tricorn Mono Q 5/50 GL column (GE Healthcare) (1 mL column volume at 1 mL/min), under the control of a Rainin HPLC system. Elution was monitored at 280 nm using a Rainin Dynamax detector and Dynamax data collection software (Rainin Instruments Inc.). The PBGS oligomers were chromatographically separated and eluted from the column using a nonlinear salt gradient of 0.02–1.0 M KCl. The buffer base was identical to that used for the 236 nm activity assay except 0.1 M HCl replaced the addition of 0.1 M ALA-HCl, unless otherwise stated. The gradient was controlled by Dynamax software. The pH 6.9 gradient consisted of 3 column volumes of 0.02 M KCl, followed by a linear increase in the concentration of KCl over 7 column volumes to 0.24 M, a plateau for 5 column volumes before another linear increase to 1.0 M KCl over 10 column volumes. The pH 9 gradient consisted of 3 column volumes of 0.02 M KCl followed by a linear gradient to 0.56 M KCl over 12 column volumes, a plateau for 5 column volumes,

a linear gradient to 1.0 M KCl over 6 column volumes, and a linear gradient to 2.0 M KCl over 10 column volumes.

Equilibrium Dialysis Experiments. Dialysis was carried out in Slide-A-Lyser dialysis cassettes (0.1–0.5 mL, 10 kDa MW cutoff, Pierce, Rockford, IL) using buffer comprised of 0.1 M BTP-HCl, 10 mM BME, 10 μM $ZnCl_2$, and 10 mM ALA-HCl. The buffer pH was 7.0 after substrate addition. Isolated heterohexamer solutions (~200 μL at 3–7 mg/mL) were dialyzed against 300 mL of buffer at 37 °C for the times indicated using gentle agitation (50–60 rpm). To ensure the continued presence of substrate, dialysis cassettes were moved into fresh dialysis buffer every 48 h. Samples were removed from the dialysis cassette at desired time points for native PAGE and mass spectrometric analyses. Protein bands were quantified by densitometry using scanned gel images and Scion Image software (Scion Corp., Frederick, MD).

Disproportionation of WT+F12L Human PBGS. The Leu12 and Phe12 content of heterohexamers and hetero-octamers during or after equilibrium dialysis was monitored as follows. Samples were removed from the dialysis cassette, and hetero-oligomers were separated by anion exchange chromatography using a Tricorn Mono Q 5/50 GL (1 mL) anion exchange column at a flow rate of 1 mL min^{-1}. The start buffer was 30 mM potassium phosphate at pH 6.5, 10 mM BME, and 10 μL of $ZnCl_2$, and the high salt buffer also contained 2.0 M KCl. The gradient consisted of a 3 column volume wash with 0.02 M KCl, followed by a linear increase in KCl concentration to 0.2 M over 9 column volumes, continued elution at 0.2 M KCl for another 9 column volumes, and a linear increase to 1.0 M KCl over 15 column volumes. Under these conditions, the heterohexamer elutes at 15.5 min (0.2 M KCl), and the hetero-octamer elutes at 25 min (0.42 M KCl). Fractions containing only heterohexamer or only hetero-octamer were pooled and concentrated to ~1 mg/mL and then dialyzed against 300 mL of 2 mM BTP-HCl buffer at pH 7.0 for 3 h to remove phosphate. The individual oligomeric forms were digested with trypsin, and the tryptic digests were analyzed by mass spectrometry to determine the Phe12 and Leu12 content of the hetero-oligomers, as we have done before (*5*).

Native Gel Electrophoresis. Native gel electrophoresis was performed as previously described (*5*), using a PhastSystem (GE Healthcare). Samples were prepared by mixing the protein solution with native gel running buffer (0.1 M Tris-HCl at pH 8.8, 20% glycerol, and 0.0025% bromphenol blue) to reach a final protein concentration of ~1 mg/mL.

Data Analysis. Data were analyzed using the programs SigmaPlot and PeakFit (Systat Software, Inc., San Jose, CA). Equations used for data fitting are described below.

$$V = \frac{V_{max} \cdot [S]_0}{K_m + [S]_0} \quad (1)$$

Where V_{max} is the velocity at saturating substrate concentration, and K_m is the substrate concentration that produces a velocity of 0.5 V_{max}.

$$V = \frac{V_{max1} \cdot [S]_0}{K_{m1} + [S]_0} + \frac{V_{max2} \cdot [S]_0}{K_{m2} + [S]_0} \quad (2)$$

Where V_{max1} and K_{m1} refer to the low K_m octameric assembly and V_{max2} and K_{m2} refer to the high K_m assemblies.

$$V = \frac{F \cdot V_{max1} \cdot [S]_0}{K_{m1} + [S]_0} + \frac{(1-F) \cdot V_{max2} \cdot [S]_0}{K_{m2} + [S]_0} \quad (3)$$

Where F is the mole fraction of subunits in the low K_m octameric assembly.

$$SA = SA_0 + a \cdot (1 - e^{-kt}) \quad (4)$$

Where SA = specific activity, SA_0 = specific activity at time 0, a = magnitude of the increase in specific activity, k = first order rate constant, and t = time.

$$SA = SA_0 + a \cdot (1 - e^{-k_1 t}) + b \cdot (1 - e^{-k_2 t}) \quad (5)$$

Equation 5 is an extension of eq 4 with a second exponential term.

$$\ln k = \ln A + \frac{E_a}{RT} \quad (6)$$

Where k is the rate constant for the reaction, E_a is the activation energy, R is the gas constant, and T is temperature (K). ln$A$ is a constant of integration.

Equation 7 was used to determine pK_a values where n is the number of protons involved.

$$SA = SA_{min} + \frac{SA_{max}}{1 + 10^{n \cdot (pH - pKa)}} \quad (7)$$

RESULTS

Rapid Interchange of Human PBGS Morpheein Forms. WT human PBGS exhibits a skewed bell shaped pH activity profile (*3*); the fit illustrated in Figure 1c is to a three proton acidic pK_a of 5.9 and a one proton basic pK_a of 8.3. Prior studies showed that the acidic pK_a is related to the binding of essential catalytic zinc ions (*12*), and the three proton curve fit is consistent with the three cysteine ligands first shown in the yeast PBGS crystal structure (*13*). The current studies address the interpretation of the basic pK_a. At pH 7.0, WT human PBGS exhibits the kinetic characteristics of a stable octamer (*1–3, 5*); plots of initial rates versus substrate concentration (10 μM−10 mM range) reflect a simple Michaelis–Menten relationship (eq 1) with one low K_m (0.2 mM) (Figure 2a). However, in the alkaline pH range, the plots fit to double hyperbolae (eq 2) indicating the presence of at least two functionally distinct human PBGS isoforms with widely different K_m values of 0.02 mM and 4.5 mM (Figure 2b and c, and refs *1–3 and 5*), where the high K_m value is identical to that obtained for hexameric F12L under these conditions (Figure 1c). The low K_m form of the WT protein corresponds to the octamer. The high K_m form is interpreted as arising predominantly from the hexamer (see SEC results below) but could also reflect contributions from either conformation of the dimer (Figure 1a). The pH dependent variation in the value of the low K_m (Figure 2d) mirrors what has been previously documented for *E. coli* PBGS (*14*).

Our past kinetic analyses of PBGS included enzyme preincubation in assay buffer and assay initiation by addition of substrate. For Figure 2a–e, K_m and V_{max} determinations were performed at pH 6.2–9.2 using Erhlich's method and initiating product formation by dilution of the enzyme into the assay. As the substrate favors the formation of the octamer, regardless of pH or protein concentration, both

methods of initiation can result in kinetic hysteresis (see below). The stock enzyme conditions (~1 mg/mL, pH 7.0) favor the octamer (Figure 2a). Thus, the high K_m forms indicated by the double hyperbolic fits illustrated at pH 8.0 (Figure 2b) and pH 8.8 (Figure 2c) appear during the 5 min assay time. To estimate the proportions of the low K_m octamer and the high K_m morpheein forms at pH 8.0 and pH 8.8, the kinetic data (e.g., Figure 2b and c) were modeled using eqs 2 and 3. Solution of eq 2 provided the K_{m1} and K_{m2} values for use in eq 3, where F and $(1 - F)$ represent the average mole fractions of the subunits in the low K_m octamer and the high K_m forms, respectively. The chosen model fixes the V_{max} of the octamer at 40 μmol h^{-1} mg^{-1} and assumes that this V_{max1} is not affected by pH in the alkaline pH range (pH 7.0–9.5). This model is consistent with the behavior of other PBGS whose allosteric magnesium stabilizes the octamer even at high pH (*15*). At pH 8.0, the solution is F (the mole fraction of human PBGS octamer) = 0.6, V_{max2} (the V_{max} of the high K_m forms) = 10 μmol h^{-1} mg^{-1}, and K_{m2} (the K_m of the high K_m forms) = 10 mM. At pH 8.8, the solution to eq 3 shows F = 0.15, V_{max2} = 5 μmol h^{-1} mg^{-1}, and K_{m2} = 5 mM. In Figure 2b and c, the solid lines are the results of modeling, and the dotted and dashed lines depict the estimated contribution of the octamer and high K_m forms, respectively. This mathematical treatment indicates that the fraction of octamer in the assay decreases with increasing pH, as illustrated in Figure 2e, where the data fit to a single pK_a of 7.8 ± 0.1, consistent with catalysis at pH 7.0, 8.0, and 8.8 by nearly all octamer, 60% octamer, and only 15% octamer, respectively. These analyses indicate that the decrease in specific activity in the alkaline pH limb of the WT human PBGS pH-specific activity profile (Figure 1c, pK_a of 8.3) can at least partially be explained by an increasing propensity to form low activity, high K_m morpheein forms. One would not expect the pK_a value attributed to reflect percent octamer (pK_a of 7.8, Figure 2e) to match that of the alkaline limb of the pH activity profile (pK_a of 8.3) as the latter reflects the sum of activites of the octamer and the high K_m species. Prior work on a synthetic human PBGS mutant, R240A, provided independent physical evidence that the hexameric assembly has increased stability at pH 9.0 relative to pH 7.0 (*4*).

The studies above suggest that human PBGS can display kinetic hysteresis, which was defined by Freiden as a slow change in enzyme activity in response to fast changes in the solution environment (e.g., ligand concentration) (*16, 17*). Although Ehrlich's assay is a sensitive and convenient means to assess PBGS activity, fixed-time assays can mask hysteresis. To detect kinetic hysteresis, the absorbance of the product, porphobilinogen, was monitored at 6 s intervals at 236 nm at pH 6.9 and pH 8.8, and is reported as specific activities (Figure 2f–h). In these assays, the enzyme (WT PBGS) was incubated in assay buffer (0.1 M BTP-HCl at pH 6.9 or pH 8.8, 1 mM TCEP-HCl, 10 μM $ZnCl_2$, and 9 mM HCl,) at 37 °C for 10 min prior to initiation of the reaction by the addition of substrate (100-fold dilution) to a final concentration of 1 mM ALA-HCl. This ALA concentration was chosen to saturate the octamer but not the high K_m components of the morpheein equilibrium. Consistent with WT human PBGS being a stable octamer under standard assay conditions, at pH 6.9, the specific activity remained constant throughout the assay (Figure 2f). In contrast, the time courses at pH 8.8 showed the enzyme very rapidly converting to low activity forms, followed by an exponential increase to plateau activity (Figure 2g). At 30 μg/mL an exponential fit (eq 4) to the data indicated a starting specific activity of 6.6 ± 0.3 μmol h^{-1} mg^{-1} and an increase in specific activity to a plateau activity of 11.1 ± 0.6 μmol h^{-1} mg^{-1}. The rate constant for this first-order increase was 0.017 ± 0.002 s^{-1}. At 100 μg/mL, the starting activity is higher, 9.4 ± 0.1 μmol h^{-1} mg^{-1}, and rose to an indistinguishable plateau activity of 10.6 ± 0.2 μmol h^{-1} mg^{-1} with a faster first-order rate constant of 0.043 ± 0.07 s^{-1}. The difference in rate constants is consistent with a protein concentration dependence to the overall hexamer-to-octamer conversion. The different initial activities at 100 μg/mL and 30 μg/mL are interpreted to indicate a PBGS-concentration dependent shift in the distribution of WT human PBGS morpheein forms upon dilution into the pH 8.8 buffer. Consistent with this finding and the modeling described above would be loss of octamer in favor of the high K_m, low activity species following dilution. The increase in activity after the addition of substrate suggests that turnover shifts the equilibria to favor octamer assembly as has been documented for the WT+F12L hetero-oligomers and for the synthetic R240A variant (*4, 5*). The time scale of the exponential increase in activity is comparable to those observed for other oligomeric enzymes that display hysteretic kinetics (*18*) and suggests that oligomer dissociation, conformational change, and alternate oligomerization may provide a plausible explanation for other hysteretic systems.

The facile nature of the WT human PBGS morpheein equilibria was also demonstrated by a pH-jump experiment illustrated in Figure 2h. In this experiment, the enzyme was preincubated at 0.1 mg/mL in pH 9.0 buffer at 37 °C prior to dilution to 10 μg/mL in pH 7.0 buffer containing 10 mM ALA-HCl at 37 °C. As shown above, under assay conditions at pH 9.0 WT human PBGS is predominantly composed of high K_m species (hexamer and/or dimers) (see Figure 2e) and almost exclusively octameric at pH 7.0 (Figure 2a). Thus, transfer from pH 9.0 to pH 7.0 would be expected to initiate an increase in specific activity as the low activity, high K_m forms of WT human PBGS convert to the high activity, low K_m octamer. This is shown in Figure 2h; the specific activity of the enzyme following dilution from pH 9.0 to pH 7.0 increased rapidly and in a biphasic manner. Fitting of the data to alternate equations, for which the residuals are presented in Figure 2i, show that the time course fit well to a double exponential function. This solution to eq 5 indicated an initial specific activity of 2.0 ± 0.6 μmol h^{-1} mg^{-1}, which is consistent with that expected for a low mole fraction of octamer, and an initial rapid increase of magnitude 22 ± 0.8 μmol h^{-1} mg^{-1}, which is interpreted to reflect an increase in the mole fraction of the octamer. The first order rate constant for this initial process is estimated to be 0.060 ± 0.005 s^{-1}. The second, slower, process is characterized by a first order rate constant of 0.005 ± 0.001 s^{-1} and a further increase in specific activity of 4.6 ± 0.5 μmol h^{-1} mg^{-1}. The double exponential increase in specific activity was observed both when the dilution was made into pH 7.0 buffer containing substrate and when dilution was made into substrate free pH 7.0 buffer and incubated at 37 °C for 10 min prior to substrate addition. Thus, a process involved in substrate turnover facilitates the conversion of the high K_m

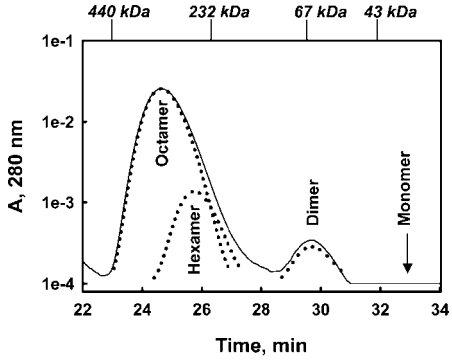

FIGURE 3: Size exclusion chromatographic analysis of the morpheein forms of WT human PBGS at pH 8.8 shows octamer, hexamer, and dimer. To enhance the perceptible dynamic range, the $A_{280\ nm}$ values (solid line) and the fitted proportions of octamer, hexamer, and dimer (dotted lines) are shown on a log scale. The expected mobility of monomer (36 kDa) is shown; the masses and mobilities of molecular weight standards are annotated above in italics.

forms of WT human PBGS (hexamer and dimers) to octamers. The biphasic nature of the increase in specific activity may be explained by an initial rate-determining re-equilibration between the morpheein forms. In this first phase, association of the pro-octamer dimer to the active octamer is not rate determining. The second slow phase is interpreted to reflect depletion of the high K_m forms such that association of dilute pro-octamer dimers to active octamer becomes rate-limiting (see Discussion).

Chromatographic Analysis of the Distribution of WT PBGS Morpheein forms. Room temperature SEC was used to demonstrate that the dimer is a stable component of the human PBGS morpheein equilibria at pH 8.8. To minimize artifacts arising from the interaction between PBGS and the column matrix, these studies required the addition of 0.1 M KCl, which stabilizes the higher order oligomers of PBGS (unpublished results). To allow high signal-to-noise UV detection of oligomeric species that exist at a low mole fraction, a 1 mg/mL sample was applied, and the data is presented on a log scale. Figure 3 illustrates that under these conditions, WT human PBGS exists as 94.7% octamer, 4.7% hexamer, and 0.6% dimer. The lower temperature, significantly higher ionic strength, significantly higher protein concentration, and the absence of substrate all differentiate the SEC conditions from the assay conditions, and thus, the ratios observed by chromatography are not expected to reflect those in the assays. However, these data demonstrate the existence of the three oligomeric stoichiometries as depicted in Figure 1 and provide the first physical evidence for the existence of stable WT human PBGS dimers. The detection limit of 0.0001 absorbance units allows us to estimate monomer contribution as no greater than 0.1%. The absence of a detectable peak for PBGS monomers is consistent with mass spectrometric analysis of heteromeric species presented later.

Anion exchange chromatography was used to further probe changes in the distribution of WT human PBGS morpheein forms in response to pH, enzyme concentration and substrate. We have previously established that octameric WT PBGS and the hexameric F12L natural variant can be separated by anion exchange chromatography at neutral pH (*3, 5*). The Mono Q chromatographic separations reported here were performed using buffer conditions chosen to mimic, as closely as possible, those used for the kinetic analyses. However, differences in temperature (37 °C vs room temperature) and ionic strength (salt gradient) can affect the morpheein equilibria; the protein also experiences dynamic changes in concentration as it adsorbs to and is eluted from the column. Despite these differences, the anion exchange chromatography results support conclusions drawn from the kinetic data described above.

Figure 4a shows the chromatographic separation of a mixture of WT and F12L human PBGS at pH 7.0 (*3, 5*). As relatively high concentrations of the two proteins were used (~3 mg/mL), the two peaks are interpreted to consist predominantly of F12L hexamer and WT octamer (as labeled). However, the dimeric variant W19A, which is not of known configuration, elutes from the Mono Q column at a position similar to that of the F12L hexamer (*4*). Hence, peaks eluting at this position are interpreted to contain an unspecified ratio of hexamer/dimer. WT PBGS eluted predominantly as octamer at pH 6.9 regardless of protein concentration. Figure 4b shows the elution profile of a stock solution of WT PBGS with a concentration of 9.6 mg/mL that was not diluted or warmed prior to loading on the column. The large peak eluting at the position of the octamer and very small peak eluting at the position of hexamer/dimer is consistent with native PAGE analyses of the sample and previous preparations (*2, 3, 5*). A 2000-fold dilution of the sample to 5 μg/mL, followed by incubation at 37 °C for 10 min prior to loading on the column reveals a 2- to 3-fold increase in the minor hexamer/dimer component (not shown). The small amount (<3%) of hexamer/dimer seen here in the absence of substrate is in agreement with a stable octamer species at pH 7.0 as indicated by the kinetic analyses above.

At pH 8.8 (Figure 4c), the F12L hexamer and WT octamer can also be resolved but require a higher ionic strength relative to pH 6.9. The F12L hexamer and WT enzyme were run separately as standards (not shown). As shown in Figure 4d, dilution of WT human PBGS to 8 μg/mL at pH 8.8 followed by incubation at 37 °C for 10 min produces a significant fraction of hexamer/dimer in the sample. The WT PBGS sample in Figure 4e has the same protein concentration as the sample in Figure 4d but was incubated with 1 mM ALA-HCl for 5 min prior to loading onto the column; the dramatic decrease in the hexamer/dimer peak and the increase in the octamer peak support our previous demonstration that catalytic turnover favors octamer (*4, 5*). However, prior work with reversible and irreversible active site directed inhibitors showed that complete turnover is not essential; some aspect of active site ligand binding appears to be sufficient (*5*). Figure 4f shows that an increased concentration of WT human PBGS (48 μg/mL vs 8 μg/mL in Figure 4d) also favors the octamer. Thus, anion exchange chromatography analyses of WT PBGS at pH 8.8 show that the octamer is less favored at pH 8.8 relative to pH 6.9, but substrate turnover still favors the octamer as does increased protein concentration.

Substrate-Mediated Equilibration of WT+F12L Hetero-Oligomers. It is established that substrate mediates an equilibrium between PBGS heterohexamers and hetero-octamers and that the position of this equilibrium is dependent on pH (*5*). The similar propensity of substrate turnover to shift the morpheein equilibria toward octamer in both WT human PBGS (Figure 2g and h) and purified WT+F12L

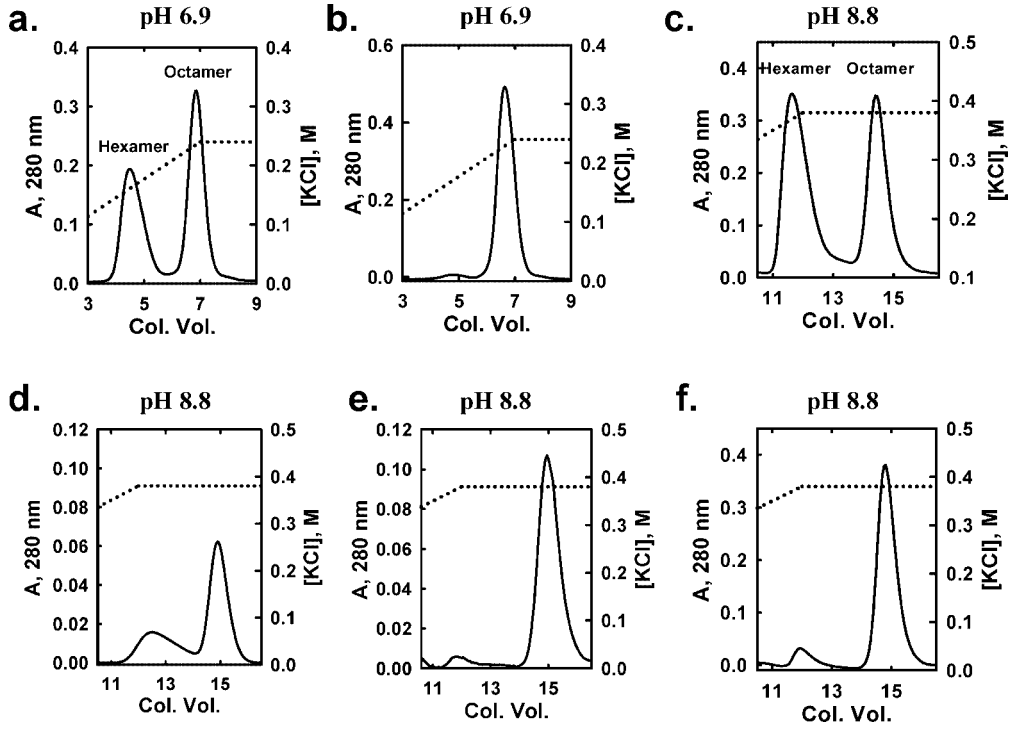

FIGURE 4: Anion exchange chromatographic analysis of the PBGS morpheein forms. The solid lines depict the $A_{280\ nm}$, and the dotted lines show the concentration of KCl. The pH values indicate the pH of the equilibration/elution buffers. (a) A mixture containing 140 μg of WT and 130 μg of F12L PBGS. (b) Forty microliters of stock WT PBGS (9.6 mg/mL). (c) A mixture of 190 μg of WT and 130 μg of F12L PBGS that was in pH 7 buffer until release from the injection loop (50 μL). (d) Five milliliters of 8 μg/mL WT PBGS that was incubated at 37 °C in 0.1 M BTP-HCl at pH 9, 10 μM $ZnCl_2$, and 1 mM TCEP-HCl for 10 min prior to loading on the column. (e) Same as in d, except that after incubation at 37 °C, ALA-HCL was added to give a concentration of 1 mM, and substrate turnover was allowed to proceed for 5 min at 37 °C before loading on to the column. (f) Same as in d, except that the concentration of WT PBGS was 48 μg/mL.

heterohexamers (*5*) suggests that the hetero-oligomeric system is a good model for the WT morpheein system. The heteromeric system has the advantage that one can isolate and store the metastable hetero-oligomers, and analysis by mass spectrometry provides insights not possible for a homomeric system. Furthermore, hetero-oligomer re-equilibration is on a time scale amenable to monitoring over a wide range of temperatures, thus we were able to construct Arrhenius plots to investigate the rate-limiting step for the conversion of heterohexamers to hetero-octamers.

Interpretation of studies on the rate of approach to equilibrium first requires definition of the effect of temperature on the equilibrium between heterohexamers and hetero-octamers. The position of the substrate-mediated equilibration between WT+F12L heterohexamers and hetero-octamers was determined at 25, 30, and 37 °C. Isolated heterohexamer was dialyzed under pH 7.0 assay conditions (with 10 mM ALA-HCl), and the morpheein equilibration process was monitored by withdrawing aliquots from the dialysis cassettes at the indicated times followed by native PAGE analyses (Figure 5a); the latest time point for each sample shows an equilibrium ratio of heterohexamers and hetero-octamers. Temperature predictably affected the rate of approach to equilibrium, but the equilibrium position attained at all three temperatures remained constant at ~50% hetero-octamer and ~50% heterohexamer.

Mass spectral analysis was used to determine the Phe12 and Leu12 content of the hetero-oligomers, which monitors the disproportionation of Phe12- and Leu12-containing subunits between heterohexamers and hetero-octamers. The hetero-oligomers were chromatographically separated and subjected to tryptic digestion and mass spectral analysis to determine the Phe12 and Leu12 content of the N-terminal tryptic peptide as described previously (*5*) and as illustrated in Figure 5b. The starting heterohexamers were comprised of 62.5% Leu12-containing subunits and 37.5% Phe12-containing subunits. After the hetero-oligomer equilibrium was reached, the percentages of Leu12-containing subunits in the resulting heterohexamers increased to 84.9%, and the Phe12-containing subunits decreased to 15.1%. Although the observed disproportionation of chains establishes that the hexamer-to-octamer transition involves dissociation of the oligomers, the mass spectral analysis did not show a 100% Leu content in the hexameric assemblies upon acheiving WT+F12L oligomeric equilibrium (Figure 5b). This is despite the propensity of Leu-12-containing subunits to disproportionate to the heterohexamers and indicates that some population of the F12L subunits, presumably those that assembled as WT+F12L heterodimers during the coexpression, was unable to exchange. To address whether disproportionation proceeds after reaching oligomeric equilibrium, disproportionation was monitored for 8 days of dialysis at 37 °C (Figure 5c). The results indicate that disproportionation continues long after establishing the heterohexamer/hetero-octamer equilibrium (Figure 5d). Nevertheless, the end point of the reaction does not indicate a hexamer population with 100% Leu12 content (89.5% Leu12 and 10.5% Phe12). We conclude that the heterodimers formed during coexpression do not exchange to form homodimers, a process that would require the formation of PBGS monomers. This is consistent with our failure to observe monomers by SEC analysis (Figure 3) and our representation of dimers as the funda-

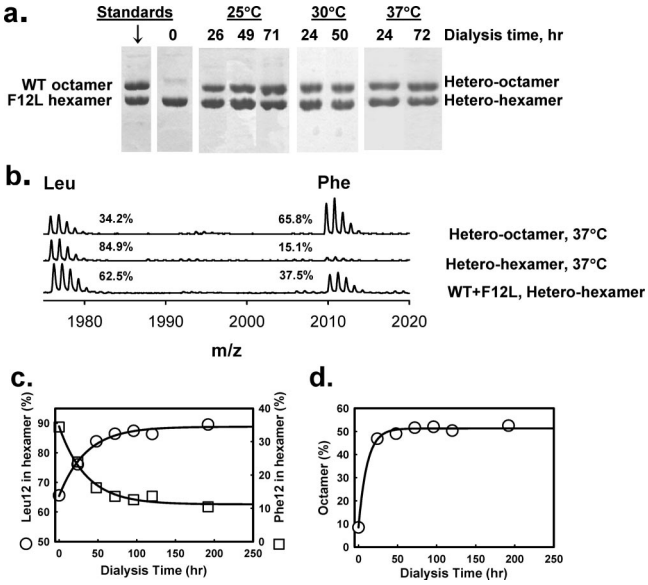

FIGURE 5: The substrate initiated re-equilibration between WT+F12L heterohexamers and hetero-octamers. (a) Native gel electrophoresis was used to determine the distribution of hetero-oligomers as a function of time and temperature during dialysis at pH 7.0 with 10 mM ALA-HCl. The far left lane shows WT and F12L as standards. The heterohexamer sample shown at zero time was used at all temperatures. (b) Mass spectral analyses before and after the turnover-moderated hexamer−octamer equilibrium was achieved shows a disproportionation of the Leu12- and Phe12-containing subunits (into the hexamer and octamer, respectively). The hetero-hexamers and hetero-octamers were chromatographically separated prior to tryptic digestion and mass spectral analysis. (c and d) Extended time course of the disproportionation of Phe12 (□)- and Leu12 (○)-containing subunits upon substrate-mediated conversion of WT+F12L heterohexamers to hetero-octamers at 37 °C. The disproportionation of subunits (panel c, determined by mass spectral analysis) proceeds long beyond attaining the oligomeric equilibrium (panel d, determined by densitometric analysis of the native PAGE results).

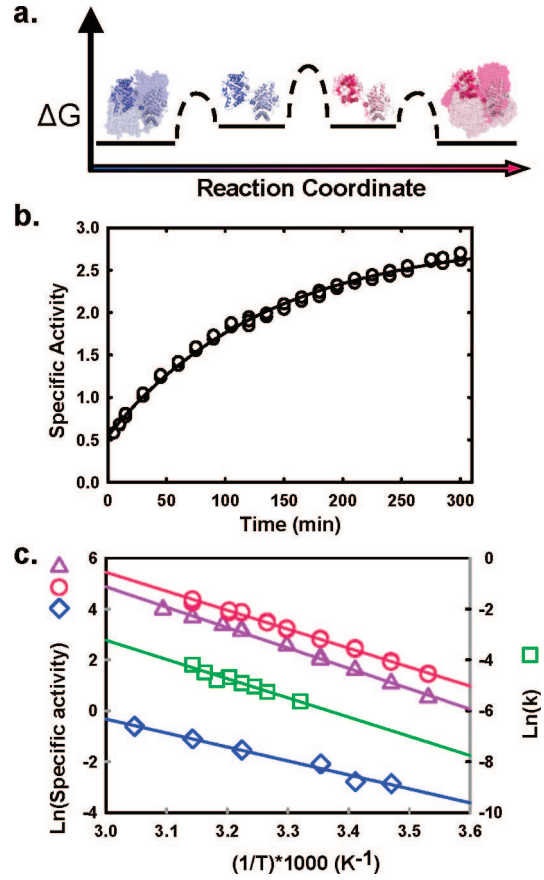

FIGURE 6: Thermodynamic analysis of the conversion of WT+F12L heterohexamers to hetero-octamers and substrate turnover by WT octamer, F12L hexamer, and WT+F12L hetero-octameric human PBGS. (a) A reaction coordinate diagram of the following equilibrium: PBGS hexamer ↔ pro-hexamer dimer ↔ pro-octamer dimer ↔ octamer. There is substantial uncertainty in the heights of the thermodynamic barriers, which are shown as dashed lines to illustrate this concept. The energy difference between the hexamer and the octamer is proposed to be small and is known to respond to the binding of ligands (*4, 5*). (b) A typical time course monitoring the increase in specific activity as the metastable heterohexamer converts to the higher activity hetero-octamer upon substrate turnover. The illustrated data were obtained at 37 °C. (c) Arrhenius plots of the first order rate constants (k, min^{-1}) for the conversion heterohexamers to hetero-octamers (green squares, right axis) and of initial rates expressed as specific activities (μmol h^{-1} mg^{-1}, left axis) of WT (red circles), F12L (blue diamonds), and WT+F12L hetero-octamers (magenta triangles). In all experiments, the concentration of ALA-HCl was 10 mM, and the pH was 7.0.

mental units of the human PBGS morpheein equilibria (Figure 1a). The apparent stability of the WT+F12L heterodimers provides further evidence that monomers are not involved in the PBGS morpheein equilibria.

Temperature Dependence of the Rate of Approach to the WT+F12L Morpheein Equilibrium. The interconversion of the WT+F12L heterohexamers and hetero-octamers requires at least three steps: oligomer dissociation, conformational change at the level of dimer, and oligomer association. Each step has specific thermodynamic properties (e.g., K_{eq} and E_a), as illustrated schematically in Figure 6a. The equilibrium position of the first and third steps, each a dissociation constant, must be protein concentration dependent (i.e., to the third power of the pro-hexamer dimer concentration and to the fourth power of the pro-octamer dimer concentration). The association rates must also be protein concentration dependent, but the association/dissociation events do not require protein backbone conformational changes. In contrast, the middle step is a protein concentration independent event that minimally requires changes in backbone and side chain conformation at several positions along the N-terminal 24 amino acids of each chain. In the absence of turnover, the WT+F12L PBGS hetero-oligomers appear stable, that is, interconversion is not observed. Re-equilibration appears to require some process that is part of catalytic turnover (e.g., some active site-based covalent inhibitors also promote hetero-oligomer equilibration (*5*)). There are no independent data addressing the rates of the first and third steps in the absence of turnover, but we can conclude that the middle step, the conformational change in the human PBGS dimer, is of low probability in the absence of active site ligands. The presence of active site ligands lowers the activation energy for the dimer interconversion step. With this in mind, the free energy of activation for the conversion of hetero-hexamers to hetero-octamers was determined and compared with the free energy of activation for substrate turnover.

To determine the free energy of activation for the conversion of heterohexamers to hetero-octamers, we took advantage of the dramatic differences in the activity of octameric (high activity) and hexameric (low activity) human PBGS at pH 7.0 (Figure 1c) (*3, 5*). Because of this difference, the transition from purified heterohexamers to a mixture of heterohexamers and hetero-octamers under turnover condi-

tions is accompanied by a progressive increase in specific activity; this process was monitored at several temperatures. Starting with purified heterohexamers (Figure 5a), the specific activity increased; this increase was fit to a first-order exponential (eq 4) as exemplified in Figure 6b (*5*). At all temperatures, the assay included a 10 min preincubation of 10 μg/mL heterohexamer in 0.1 M BTP-HCl at pH 7.3, 10 μM $ZnCl_2$, and 10 mM BME, and the reaction was initiated by the addition of a temperature equilibrated aliquot of 0.1 M ALA-HCl to a final concentration of 10 mM (which brought the final pH to 7.0). The time courses for the conversion of heterohexamer to hetero-octamer were monitored by periodically removing aliquots from the incubations and immediatly quantifying porphobilinogen using Ehrlich's reagent and calculating specific activities based on the total incubation time. Rate constants, obtained over the range of 28–45 °C, are presented as an Arrhenius plot (Figure 6c). The Arrhenius plot is linear over the range of temperatures employed, which suggests that the rate-limiting step is the same at all temperatures. An activation energy for heterohexamer to hetero-octamer conversion ($E_a = 63 \pm 5$ kJ/mol) was determined from the slope of the plot (eq 6). The contributions of the individual processes to the energy barrier for conversion of hexamer to octamer are unknown. However, we previously monitored this process at 5 μg/mL and 0.9 mg/mL, two widely different enzyme concentrations, by specific activity increase and dynamic light scattering, respectively. The observed identical rates of approach to equilibrium (*5*) indicate that the rate of heterohexamer-to-hetero-octamer conversion is independent of protein concentration. In the direction from heterohexamers to hetero-octamers, the hexamer dissociation process and the internal dimer conformational change process are expected to be independent of protein concentration, suggesting that one of these is the rate-determining process.

Activation Energy for Catalysis by WT, F12L, and WT+F12L Hetero-Octameric Human PBGS. As some aspect of substrate turnover is a prerequisite for the conversion of metastable heterohexamers to hetero-octamers, the free energies of activation for substrate turnover by WT octamer, F12L hexamer, and WT+F12L hetero-octameric human PBGS were determined. Assay conditions were the same as those used to determine the activation energy for conversion of heterohexamers to hetero-octamers (pH 7.0, 10 mM ALA-HCl). The Arrhenius plots from whose slope the activation energies were derived, using eq 6, are shown in Figure 6c. The activation energies for substrate turnover by WT octamer and WT+F12L hetero-octamer were determined to be 62 $\pm$ 1 kJ/mol and 67 $\pm$ 1 kJ/mol, respectively, values that are remarkably similar to that for the conversion of heterohexamers to hetero-octamers. However, for the F12L variant, a lower activation energy of 45 $\pm$ 3 kJ/mol for substrate turnover was obtained, indicating that the rate-limiting step in catalysis by the PBGS hexamer is different from that for catalysis by the PBGS octamer and different from the rate-limiting step for the heterohexamer-to-hetero-octamer conversion. Our interpretation of the similarities and differences of these activation energies is discussed below.

DISCUSSION

Composition of the Human PBGS Morpheein Equilibria. The propensity of to exist as an equilibrium of morpheein forms, with different oligomeric multiplicity and functionality, is now well established (*1–5*). However, Figure 7 illustrates how the current view (Figure 1a) uses different models, which are derived from crystal structures 1E51 and 1PV8, for the physiologically relevant dimers. Our prior work presented the asymmetric units in the crystal structure as the solution structures of the interchanging dimers (*3–5*). These hugging and detached dimers (Figure 7a and b, respectively) each contain exposed hydrophobic surface patches that become buried in the higher order oligomers. Our previous model considered these dimers as transient intermediates. Increasing evidence for stable WT dimers in solution (Figure 3) and increasing consideration for the importance of water in protein interfaces (*19, 20*) caused the consideration of alternate dimer structures. The current view describes dimer structures (Figure 7c and d) that do not expose hydrophobic surface patches. The solvent accessible surfaces of these newly named pro-octamer and pro-hexamer dimers are characterized in the crystal structure of the oligomer by intersubunit hydrogen bonds, ion pairs, and ordered water molecules. For example, Figure 7e shows the hydrophilic nature of the interface between one pro-hexamer dimer and the rest of the protein, as extracted from the crystal structure of human PBGS variant F12L. The dissociation of either the octamer into pro-octamer dimers or the hexamer into pro-hexamer dimers is proposed to be a low-activation energy process because the dissociating intersubunit surfaces are predominantly hydrophilic in nature and already contain many ordered water molecules (Figure 7e). In the current presentation, the pro-hexamer and pro-octamer dimers are considered to be stable entities that exist in a protein concentration dependent equilibrium with their respective oligomers in solution; Figure 3 provides physical evidence for the existence of free dimers, but no evidence for free monomers. Dissociation to monomer is expected to be a rare event that would expose significant hydrophobic patches to bulk solvent. Consistent with this expectation is the lack of interchange between the subunits of heterodimers containing both Phe12 and Leu12 implied from a WT+F12L heterohexamer disproportionation study (Figure 5c); such an interchange would require the existence of free monomers.

Rate-Limiting Step for Morpheein Interconversion. The close similarity of the activation energies for the conversion of WT+F12L PBGS heterohexamers to hetero-octamers with the activation energies for catalysis by both the WT PBGS octamer and the WT+F12L hetero-octamers (Figure 6c) suggests that these processes share the same rate-limiting event. This common event is reasoned below to involve structural changes in the active site lid. Catalysis by the PBGS octamer involves sequential binding of the two substrate molecules (the first one as a Schiff base), closing of the active site lid, a series of additional bond-breaking and bond-making steps to produce a product-like intermediate, active site lid opening, and finally product release (*8*). Because human PBGS isolates with product (or some near-product intermediate (*8, 21*)) bound in one-half of the active sites (*22*) and because this product does not release until the substrate interacts with the open active sites, we conclude that lid opening to allow product release is part of a reciprocating action in response to substrate binding and lid closing in an adjacent subunit (*8, 23*). The reciprocating

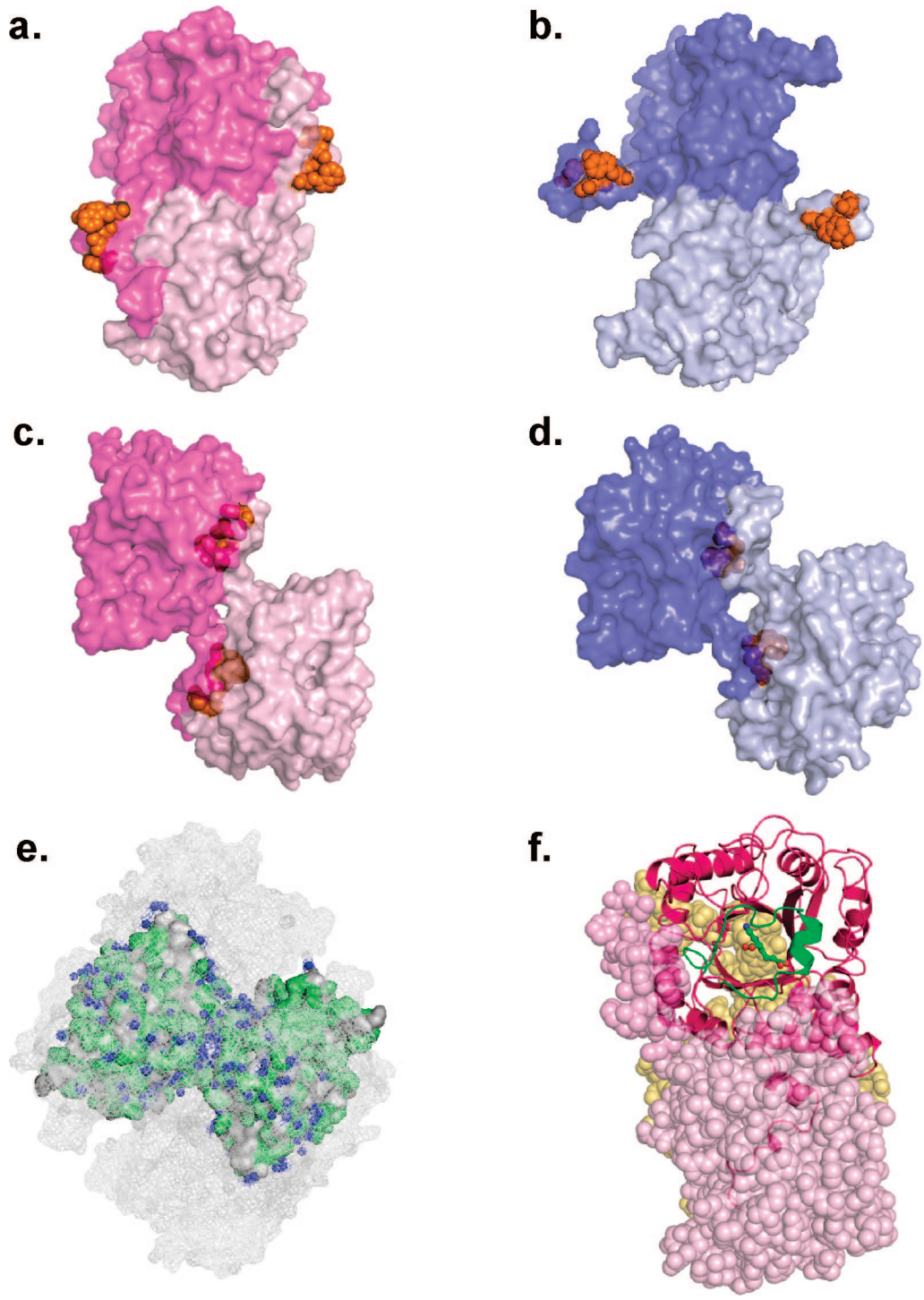

FIGURE 7: Alternate views of human PBGS structures and the physiologically relevant dimer assemblies of human PBGS. (a) The asymmetric unit in the crystal structure of WT human PBGS is the hugging dimer (*22*), which contains exposed hydrophobic patches (orange). (b) The asymmetric unit of the PBGS hexamer crystal structure of the human PBGS F12L variant is the detached dimer (*3*), which also contains exposed hydrophobic patches (orange). (c) The pro-octamer dimer with the main hydrophobic patch (orange, Leu15, Leu16, and Trp19) buried within the dimer interface. (d) The pro-hexamer dimer with the main hydrophobic patch (orange) buried within the dimer interface. (e) Hydration of the oligomeric interface of the F12L human PBGS hexamer. The pro-hexamer dimer is shown in surface representation with the charged and polar residues colored green. Water molecules within 4 Å of this surface are shown as blue spheres. The remaining subunits of the hexamer are shown as a mesh. (f) The active site of the WT human PBGS octamer is illustrated within the context of the three subunits that interact at one active site. Subunit A is shown as a dark pink cartoon, with the active site lid in green. Porphobilinogen is shown (colored as in Figure 1e) in the α/β-barrel of subunit A. Subunit B (light pink spheres) is the partner of subunit A in the hugging dimer. The arm from subunit F (yellow spheres) excludes solvent from the back of the barrel; subunit F is the partner of subunit A in a pro-octamer dimer.

motion model is particularly well supported by biochemical analysis of PBGS from *Drosophila melanogaster* (*23*).

The rate-determining process in the conversion of hetero-hexamer to hetero-octamer is a protein concentration independent event (see above). On the basis of the sequence of events illustrated in Figure 6a, such an event *could* be hexamer dissociation or the dimer interconversion steps; but it is not reasonable to propose that either of these events is

an *obligate* component of catalysis by PBGS octameric assembly. Thus, the rate-limiting event is an alternative unimolecular process, common to catalysis by the octamer (homo or hetero) and to the heterohexamer-to-hetero-octamer interconversion, not explicitly noted in Figure 6a. Furthermore, this rate-limiting event is not part of the hexameric catalytic cycle because the activation energy for catalysis by the F12L hexamer is significantly lower.

With these criteria in place, comparison of the crystal structures used to assemble the reaction coordinate for oligomer interconversion (Figure 6a) reveals two significant changes that occur on moving from the hexamer to the octamer. These are (1) a twist between the two barrel domains of the pro-oligomer dimers (best seen in Figure 1b) and (2) the greater degree of order found in the active site lids of four of the subunits in the octamer (detailed in Figure 1d and e). The dimeric twist event is the distinct conformational change that determines whether dimers associate to hexamers or octamers and thus may be regarded as the distinguishing feature between the two dimers. In the octamer crystal structure, where product is modeled to the electron density observed at one-half of the active sites, those four lids are ordered in a closed conformation; for the vacant active sites, the active site lids of the octamer are disordered. This suggests that the substrate assists in closing the lid. In the hexamer crystal structure, where the electron density indicates a bisubstrate intermediate at one-half of the active sites, all six of the active site lids are disordered, suggesting that substrate binding alone is not sufficient to close the active site lid. Thus, a fully stable closed lid conformation has two requirements: (1) that the carboxylic acid moiety of the K_m determining ALA must be present to interact with Arg209 and Arg221 on the lid (see Figure 1e) and (2) that the octameric assembly must be in place so that the lid-stabilizing arm-to-barrel interaction exists. Figure 7f illustrates one active site in the octameric assembly and shows how three subunits contribute to the active site environment. One subunit contains the catalytic residues in the center of its $\alpha\beta$-barrel. The N-terminal arm of a second subunit fits snugly into the back of this $\alpha\beta$-barrel excluding solvent access from the back. The third subunit provides the arm-to-barrel interaction that stabilizes the active site lid, thus excluding solvent access from the front. This last interaction is not present in the hexamer.

The PBGS crystal structures (Figure 1 and Figure 6a) can be used to address possible rate-limiting events that are not explicitly depicted in the hexamer-to-octamer reaction coordinate diagram (Figure 6a). The crystal structures reflect the higher order oligomers; thus, we have no independent data on the order/disorder of the active site lids in the fully dissociated dimeric assemblies. Furthermore, we cannot discriminate whether lid closure can or does occur in the dimeric assemblies. One possibility is that lid closure is a rare event in the dimeric assemblies and occurs primarily after pro-octamer dimers associate to octamer and active site ligands bind. An alternative scenario is that lid closure is a favorable conformation in the normal equilibrium of structures regularly sampled by the active site lid and can readily occur in the pro-octamer dimer prior to octamer formation. In the latter scenario, transient closure of the lid does not *require* the hugging arm-to-barrel interaction that is only present in the fully assembled octamer (Figure 7f). In either scenario, it is the opening and/or closing of the active site lid that constitutes a unimolecular event common to octamer catalysis and heterohexamer-to-hetero-octamer conversion but separate from catalysis by the hexamer. However, we do not know where this rate-limiting event occurs in the reaction coordinate.

How Morpheein Equilibria Affect the Determination of an Enzyme Catalyzed Reaction Mechanism. The studies on WT human PBGS reported herein arose from a desire to use solvent isotope effects to probe the mechanism of the PBGS catalyzed reaction, which involves the overall loss of four protons to water and which suggests that determination of deuterium or tritium isotope effects might provide significant mechanistic information. However, the precision required for meaningful interpretation of isotope effect data requires that the enzyme exist as a single stable species that utilizes a uniform enzymatic mechanism under all assay conditions (e.g., different pH conditions). Ensuring such uniformity of structure and mechanism for an enzyme that has morpheein forms is shown herein to be complex. Factors that can perturb a morpheein equilibrium include, but are not limited to, enzyme concentration, substrate concentration, pH, temperature, ionic strength, and solvent isotope composition (e.g., H_2O/D_2O). Failure to account for such changes can result in erroneous, unexplainable, and/or misinterpreted data. For example, the basic pK_a seen in Figure 1c is not attributed to the titration of an essential active site amino acid, but rather reflects the pH dependent increase in the hexameric assembly of WT human PBGS (Figure 2g). Although other pH rate profiles have been interpreted to reflect conformational changes, PBGS provides an outstanding example of a pH rate profile that reflects a quaternary structure change. Another example appears to be phosphofructokinase, where the acidic limb of the pH rate profile has been interpreted to reflect an equilibrium between active tetramers and inactive dimers (*24–26*).

Summary. Human PBGS exists in a set of dynamic equilibria between hexamer, pro-hexamer dimer, pro-octamer dimer and octamer, where the difference between the ground-state energies for the oligomers is small enough that all forms can be present in measurable amounts in solution. Our present understanding of the thermodynamics of the human PBGS morpheein ensemble, depicted in Figure 6a, does not reveal the precise step during which the rate-determining active site lid opening/closing event occurs. The structures of the newly realized pro-hexamer and pro-octamer dimers allow association and dissociation to occur without significant hydration/dehydration of the exposed/buried surfaces. In addition to determining the central importance of active site lid motion in PBGS function, we present strong evidence supporting the hypothesis that the basic arm of the human PBGS pH rate profile is dominated by changes in the quaternary structure.

ACKNOWLEDGMENT

We acknowledge Ms. Linda Stith for purification of WT human PBGS and Dr. Yibai Chen (Fox Chase Cancer Center, Mass Spectrometry Facility) for collecting mass spectrometry data.

REFERENCES

1. Jaffe, E. K. (2005) Morpheeins: a new structural paradigm for allosteric regulation. *Trends Biochem. Sci. 30*, 490–497.

2. Jaffe, E. K., and Stith, L. (2007) ALAD porphyria is a conformational disease. *Am. J. Hum. Genet. 80*, 329–337.
3. Breinig, S., Kervinen, J., Stith, L., Wasson, A. S., Fairman, R., Wlodawer, A., Zdanov, A., and Jaffe, E. K. (2003) Control of tetrapyrrole biosynthesis by alternate quaternary forms of porphobilinogen synthase. *Nat. Struct. Biol. 10*, 757–763.
4. Tang, L., Breinig, S., Stith, L., Mischel, A., Tannir, J., Kokona, B., Fairman, R., and Jaffe, E. K. (2006) Single amino acid mutations alter the distribution of human porphobilinogen synthase quaternary structure isoforms (morpheeins). *J. Biol. Chem. 281*, 6682–6690.
5. Tang, L., Stith, L., and Jaffe, E. K. (2005) Substrate-induced interconversion of protein quaternary structure isoforms. *J. Biol. Chem. 280*, 15786–15793.
6. Petrotchenko, E. V., Pedersen, L. C., Borchers, C. H., Tomer, K. B., and Negishi, M. (2001) The dimerization motif of cytosolic sulfotransferases. *FEBS Lett. 490*, 39–43.
7. Xu, Q., Canutescu, A., Obradovic, Z., and Dunbrack, R. L., Jr. (2006) ProtBuD: a database of biological unit structures of protein families and superfamilies. *Bioinformatics 22*, 2876–2882.
8. Jaffe, E. K. (2004) The porphobilinogen synthase catalyzed reaction mechanism. *Bioorg. Chem. 32*, 316–325.
9. Jaffe, E. K., Martins, J., Li, J., Kervinen, J., and Dunbrack, R. L., Jr. (2001) The molecular mechanism of lead inhibition of human porphobilinogen synthase. *J. Biol. Chem. 276*, 1531–1537.
10. Jordan, P. M., and Gibbs, P. N. (1985) Mechanism of action of 5-aminolaevulinate dehydratase from human erythrocytes. *Biochem. J. 227*, 1015–1020.
11. Huckel, D., and Beyersmann, D. (1979) Rapid purification and direct spectrophotometric assay for 5-aminolevulinic acid dehydratase. *Anal. Biochem. 97*, 277–281.
12. Jaffe, E. K., Volin, M., Bronson-Mullins, C. R., Dunbrack, R. L., Jr., Kervinen, J., Martins, J., Quinlan, J. F., Jr., Sazinsky, M. H., Steinhouse, E. M., and Yeung, A. T. (2000) An artificial gene for human porphobilinogen synthase allows comparison of an allelic variation implicated in susceptibility to lead poisoning. *J. Biol. Chem. 275*, 2619–2626.
13. Erskine, P. T., Senior, N., Awan, S., Lambert, R., Lewis, G., Tickle, I. J., Sarwar, M., Spencer, P., Thomas, P., Warren, M. J., Shoolingin-Jordan, P. M., Wood, S. P., and Cooper, J. B. (1997) X-ray structure of 5-aminolaevulinate dehydratase, a hybrid aldolase. *Nat. Struct. Biol. 4*, 1025–1031.
14. Mitchell, L. W., Volin, M., and Jaffe, E. K. (1995) The phylogenetically conserved histidines of *Escherichia coli* porphobilinogen synthase are not required for catalysis. *J. Biol. Chem. 270*, 24054–24059.
15. Kervinen, J., Dunbrack, R. L., Jr., Litwin, S., Martins, J., Scarrow, R. C., Volin, M., Yeung, A. T., Yoon, E., and Jaffe, E. K. (2000) Porphobilinogen synthase from pea: expression from an artificial gene, kinetic characterization, and novel implications for subunit interactions. *Biochemistry 39*, 9018–9029.
16. Frieden, C. (1970) Kinetic aspects of regulation of metabolic processes. The hysteretic enzyme concept. *J. Biol. Chem. 245*, 5788–5799.
17. Frieden, C. (1979) Slow transitions and hysteretic behavior in enzymes. *Annu. Rev. Biochem. 48*, 471–489.
18. Kurganov, B. I., Dorozhko, A. K., Kagan, Z. S., and Yakovlev, V. A. (1976) The theoretical analysis of kinetic behaviour of "hysteretic" allosteric enzymes. I. The kinetic manifestations of slow conformational change of an oligomeric enzyme in the Monod, Wyman and Changeux model. *J. Theor. Biol. 60*, 247–269.
19. Teyra, J., Doms, A., Schroeder, M., and Pisabarro, M. T. (2006) SCOWLP: a web-based database for detailed characterization and visualization of protein interfaces. *BMC Bioinf. 7*, 104.
20. Teyra, J., and Pisabarro, M. T. (2007) Characterization of interfacial solvent in protein complexes and contribution of wet spots to the interface description. *Proteins 67*, 1087–1095.
21. Erskine, P. T., Coates, L., Butler, D., Youell, J. H., Brindley, A. A., Wood, S. P., Warren, M. J., Shoolingin-Jordan, P. M., and Cooper, J. B. (2003) X-ray structure of a putative reaction intermediate of 5-aminolaevulinic acid dehydratase. *Biochem. J. 373*, 733–738.
22. Mills-Davies, N. L. (2000) Structure of Human Erythrocyte 5-Aminolaevulinic Acid Dehydratase, The Second Enzyme in the Biosynthesis Pathway of Haem, Ph.D. Thesis, University of Southampton, Southampton, U.K.
23. Kundrat, L., Martins, J., Stith, L., Dunbrack, R. L., Jr., and Jaffe, E. K. (2003) A structural basis for half-of-the-sites metal binding revealed in *Drosophila melanogaster* porphobilinogen synthase. *J. Biol. Chem. 278*, 31325–31330.
24. Hofer, H. W., and Krystek, E. (1975) Determination of the kinetic parameters of phosphofructokinase dissociation. *FEBS Lett. 53*, 217–220.
25. Pavelich, M. J., and Hammes, G. G. (1973) Aggregation of rabbit muscle phosphofructokinase. *Biochemistry 12*, 1408–1414.
26. Su, J. Y., and Storey, K. B. (1995) Fish muscle phosphofructokinase: Influences of protein concentration on enzyme kinetic behaviour. *Int. J. Biochem. Cell Biol. 27*, 1277–1283.

BI702113Z